Revista de la Facultad de Ciencias Universidad Nacional de Colombia, Sede Medellín
V 11 N°1 enero-junio de 2022 • ISSN-e 2357-5749 • Artículo Investigación • Páginas 17 a 39
DOI: https://doi.org/10.15446/rev.fac.cienc.v11n1.97719

EVALUATION OF THREE LIGNOCELLULOSE BIOMASS MATERIALS (BARLEY HUSK, CORN COBS, AGAVE LEAVES) AS PRECURSORS OF ACTIVATED CARBON[a]

EVALUACIÓN DE TRES MATERIALES DE BIOMASA LIGNOCELULOSICA (CÁSCARA DE CEBADA, MAZORCAS DE MAÍZ, HOJAS DE AGAVE) COMO PRECURSORES DEL CARBÓN ACTIVADO

ROBERTO A. CANALES-FLORES[b], FRANCISCO PRIETO-GARCÍA[b *], JUDITH PRIETO-MÉNDEZ[b], OTILIO A. ACEVEDO-SANDOVAL[b], ELENA M. OTAZO-SÁNCHEZ[b]

Recibido 09-08-2021, aceptado 26-12-2021, versión final 30-12-2021
Research paper

ABSTRACT: Lignocellulosic biomass is a promising alternative and renewable energy source that can be transformed into other value-added products such as activated carbon. The objective was to evaluate the barley husk (*Hordeum vulgare* L.), the corn cobs (*Zea Mays* L.) and the agave leaves (*Agave salmiana*) as potential precursors of activated carbon. These precursors were obtained from Almoloya and Apan in the State of Hidalgo, Mexico. The raw materials were washed with distilled water, dried at 105°C for 72 h in an oven, ground in a blade mill to obtain a particle size of 0.3 – 1.0 mm and finally sieved through mesh sieves of 18 and 45. Humidity was determined according to ASTM D3173 (ASTM Standard D3173, 1996), ash according to ASTM D3174 (ASTM Standard D3174, 2000) , volatile matter according to ASTM D3175 (ASTM Standard D3175, 1997), fixed carbon according to ASTM D3172 (ASTM Standard D3172, 1997), total sugars and fats according to TAPPI T204 (TAPPI, 1997), Klason Lignin according to TAPPI T222 (TAPPI, 1998), holocellulose according to the method described by Wise *et al.* (1946), and α, β y γ cellulose according to TAPPI T203 (TAPPI, 1999). The results show that contents from 82 to 83 % for holocellulose, from 52 to 79 % for cellulose, and from 15 to 26 % for lignin, were determined. Elemental analysis showed high carbon contents with values of 42-45 %. Particle sizes between 390.9 μm and 610.7 μm were found. Thermogravimetric analysis showed similar profiles of thermal decomposition, being cellulose the main stage, with peaks around 300°C. Regarding the surface morphology, the lignocellulosic residues showed fibrous and porous structure. From these findings, it is established that the precursors analyzed can be considered as potential precursors of activated carbons. The results presented here may facilitate improvements in the pyrolysis and activation areas of this lignocellulosic residues. The conditions for an acceptable yield of biochar were tested, these were: carbonization temperature of 400°C, carbonization time of 30 min, precursor mass of 2 – 10 g and N_2 flow rate of $150 cc/min$. The biocarbons produced under these conditions were physically and chemically characterized. Biochar yields of 19.75 % were obtained for corn cob (CCB), 32.88 % for barley husk (BHB) and 31.14 % for *Agave salmiana* leaves (ALB). Biocarbons with a

---

[a] Canales-Flores, R. A., Prieto-García, F., Prieto-Méndez, J., Acevedo-Sandoval, O. & Otazo-Sánchez, E. (2022). Evaluation of three lignocellulose biomass materials (barley husk, corn cobs, agave leaves) as precursors of activated carbon. *Rev. Fac. Cienc.*, 11 (**1**), 17–39. DOI: https://doi.org/10.15446/rev.fac.cienc.v11n1.97719

[b] Academic Area of Chemistry, Autonomous University of Hidalgo State, México

[*] Autor para la correspondencia: prietog@uaeh.edu.mx

predominantly macroporous structure, amorphous structure, numerous oxygen functional groups, anionic surface and moderate ash content were obtained. The results of this investigation show that barley husk, corn cob, and agave leaves are likely precursors for biochar production with good dye adsorption capacities.

KEYWORDS: Activated carbon; Barley husk; Corn cob; Agave leaves; Lignocellulosic materials; Biomass; Thermogravimetry.

RESUMEN: La biomasa lignocelulósica es una prometedora fuente de energía alternativa y renovable que puede transformarse en otros productos de valor añadido como el carbón activado. El objetivo fue evaluar la cáscara de cebada (*Hordeum vulgare* L.), las mazorcas de maíz (*Zea Mays* L.) y las hojas de agave (*Agave salmiana*) como potenciales precursores del carbón activado. Estos precursores se obtuvieron de Almoloya y Apan en el Estado de Hidalgo, México. Las materias primas se lavaron con agua destilada, se secaron a 105 ºC durante 72 h en un horno, se molieron en un molino de cuchillas para obtener un tamaño de partícula de $0.3-1.0$ mm y finalmente se tamizaron a través de tamices de malla de 18 y 45. La humedad se determinó de acuerdo con la Norma ASTM D3173 (ASTM Standard D3173, 1996), cenizas según la Norma ASTM D3174 (ASTM Standard D3174, 2000), materia volátil según la Norma ASTM D3175 (ASTM Standard D3175, 1997), carbono fijo según la Norma ASTM D3172 (ASTM Standard D3172, 1997), azúcares y grasas totales según el TAPPI T204 (TAPPI, 1997), Lignina Klason según el TAPPI T222 (TAPPI, 1998), holocelulosa según el método descrito por Wise *et al.* (1946), y α, β y γ celulosa según el TAPPI T203 (TAPPI, 1999). Los resultados muestran que se determinaron contenidos de 82 % a 83 % para holocelulosa, de 52 % a 79 % para celulosa y de 15 % a 26 % para lignina. El análisis elemental mostró altos contenidos de carbono con valores de 42-82 %. Se encontraron tamaños de partículas entre 390.9 μm y 610.7 μm. El análisis termogravimétrico mostró perfiles similares de descomposición térmica, siendo la celulosa el escenario principal, con picos alrededor de los 300°C. En cuanto a la morfología superficial, los residuos lignocelulósicos mostraron estructura fibrosa y porosa. A partir de estos hallazgos, se establece que los precursores analizados pueden considerarse como potenciales precursores de los carbones activados. Los resultados presentados aquí pueden facilitar mejoras en las áreas de pirólisis y activación de estos residuos lignocelulósicos. Se probaron las condiciones para un rendimiento aceptable de biocarbón, estas fueron: temperatura de carbonización de 400°C, tiempo de carbonización de 30 min, masa de precursor de $2-10$ g y caudal de N_2 de $150 cc/min$. Los biocarbonos producidos en estas condiciones se caracterizaron física y químicamente. Se obtuvieron rendimientos de biocarbón de 19.75 % para mazorca de maíz (CCB), 32.88 % para cáscara de cebada (BHB) y 31.14 % para hojas de *Agave salmiana* (ALB). Se obtuvieron biocarbonos de estructura predominantemente macroporosa, estructura amorfa, numerosos grupos funcionales oxígeno, superficie aniónica y contenido moderado de cenizas. Los resultados de esta investigación muestran que la cáscara de cebada, la mazorca de maíz y las hojas de agave son probablemente precursores de la producción de biocarbón con buenas capacidades de adsorción de colorantes.

PALABRAS CLAVE: Carbón activado; cáscara de cebada; mazorca de maíz; hojas de agave; materiales lignocelulósicos; biomasa; termogravimetría.

1. INTRODUCTION

Biomass is a complex biological organic or non-organic solid product derived from living or living organism and available naturally (Tripathi *et al.*, 2016). Lignocellulosic biomass is considered a promising alternative and renewable energy source that can be transformed by pyrolysis process into other value-added products such as activated carbon and bio-oil (Stefanidis *et al.*, 2014).

Significant research have been devoted to the production of activated carbons from agricultural residues because of availability and low cost (Canales-Flores & Prieto-García, 2016). Wood, corn straw, olive stones, bagasse, sugar cane bagasse, almond shells, corn stover, apricot stones, nut shells, corn cob, rice husk and rice straw are some examples of biomass used for obtaining activated carbons (Canales-Flores & Prieto-García, 2016). Other studies have shown that the microporous structure and chemical surface of activated carbon as well as high carbon content make it useful for several industrial applications (Xiao *et al.*, 2012; Tripathi *et al.*, 2016). Thus, in agriculture industry it is used to upgrade the soil quality, in purification industry it is used to remove heavy metals, and in textile industry it is used to dye removal (Tripathi *et al.*, 2016). According to Tripathi *et al.* (2016), the production of activated carbons from the biomass does not only depend upon the process employed to produce but it is also a function of the process parameters involved in the production also. In recent years, several researchers have focused on the obtaining of carbonaceous materials from lignocellulosic biomass. They have shown that the production and properties of activated carbon depends upon several factors like biomass properties (type of biomass, moisture content, particle size and chemical composition), reaction conditions and other factors (Cagnon *et al.*, 2009; Tripathi *et al.*, 2016). Regarding biomass properties, lignocellulosic biomass is composed mainly of three basic structural components: cellulose, hemicellulose, and lignin (Khezami *et al.*, 2005; Azevedo *et al.*, 2013; Stefanidis *et al.*, 2014). Cellulose is the main component, is a linear polysaccharide constituted by long chains of glucose residues. Its composition is C: 44.4 %, O: 49.4 % and H: 6.2 % in weight (Tripathi *et al.*, 2016). Hemicelluloses are relatively low-molecular weight non-cellulosic polysaccharides. Its elemental composition is about the same as that of cellulose. Lignin is a three-dimensional polymer made of phenylpropane units. Its composition is C: 62 %, O: 32 % and H: 6 % in weight, which differs from that of cellulose (Khezami *et al.*, 2005). In addition to these components, lignocellulosic biomass also contains a small amount of inorganic material (ash) and extractives (Stefanidis *et al.*, 2014); The content of cellulose, hemicellulose and lignin in biomass varies depending on the biomass type (Stefanidis *et al.*, 2014). Several literatures are available discussing the effect of biomass constituents on the activated carbon production. In this study, the objective was to evaluate the barley husk (*Hordeum vulgare* L.), corn cobs (*Zea Mays* L.) and agave leaves (*Agave salmiana*) as potential precursors of activated carbon.physical and chemical characterization of barley husk, corn cobs and agave leaves were discussed to evaluate its potential as precursors of activated carbons. This would be the first study that is reported with the use of *Agave salmiana* leaves as a precursor in obtaining activated carbons. This constitutes a novel part of this work and this hipothesy may be of interest to other regions of the world where *agavaceae* are cultivated. Therefore, it is assumed that the production of biochar from barley husk, corn cob and leaves of *Agave salmiana* by pyrolysis in a muffle furnace is possible.

2. MATERIALS AND METHODS

The lignocellulosic residues utilized in this study were obtained from Barley husk (BH), corn cobs (CC) and *Agave salmiana* (AS) collected in Almoloya and Apan in the State of Hidalgo, México. The raw materials were washed five times with distilled water, titrated in a food processor, dried at 105 ºC for 72 h in an oven, ground in a knife mill to obtain 0.3-1.0 mm particle size and finally sieved through 18 and 45 mesh sieves.

Moisture was determined according to the ASTM Standard D3173 (1996), ash according to the ASTM Standard D3174 (2000), volatile matter according to the ASTM Standard D3175 (1997), fixed carbon according to the ASTM Standard D3172 (1997), total sugars and fat according to the TAPPI (1997), Klason lignin according to the TAPPI (1998), holocellulose according to the method described by Wise *et al.* (1946), and α-, β- and γ- cellulose according to the TAPPI (1999).

The raw materials were characterized by elemental analyses to know the content of C, H and N, laser diffraction particle size to analyze particle sizes distribution, thermogravimetry to study the transformations occurring in the precursor during carbonization, Fourier Transform infrared spectrophotometry to obtain information on the presence of functional groups, and scanning electron microscopy to observe the surface morphology of the precursors.

Particle sizes distribution of the precursors materials was determined with a Beckman Coulter laser diffraction particle size analyzer model LS13-320. Elemental analyses of C, H and N of dried samples were performed using a Perkin Elmer analyzer model 2400 PECHN-SO using acetanilide as the reference. The oxygen content was obtained indirectly by difference.

The thermal behavior of the lignocellulosic precursors was performed with a Mettler-Toledo analyzer model TGA/SDTGA-851, under a nitrogen atmosphere, with a heat ramp of 10 ºC min^{-1} up to 600 ºC.

Spectra were recorded in a Perkin Elmer Spectrum one spectrometer. The samples were mixed with KBr powder and the mixture was pressed into pellet. The spectra were recorded in the region of 4000 to 370 cm^{-1}, resolution of 4 cm^{-1} and 10 scans.

The surface morphology of the precursors materials was observed by means of SEM using a JEOL scanning electron microscope model JSM 6300 operated at 10 kV. For observation, particles of the precursors were dispersed onto carbon tape and coated with gold.

An AutoPore IV 9500 porosimeter (Micromeritics) was used, evacuated at a pressure of approximately 7.10-6 MPa ($50 \mu mHg$), followed by filling with mercury at a pressure of 413.68 MPa. The pore size distribution was determined as proposed in the literature (Weber *et al.*, 2010).

The preparation and characterization of the biofuels was carried out by carbonizing the three precursors in a muffle furnace with nitrogen gas circulation with purity of 99.999 % to completely purge the air from the reaction environment for 30 minutes and allow the pyrolysis process. The temperature of the muffle was raised at a constant heating rate of 20°C / min until reaching the final carbonization temperature of 400°C. The system was kept at the carbonization temperature during the carbonization time and finally, the system was cooled to room temperature under nitrogen flow and the biochar obtained was removed from the furnace. The yield of biochar production was calculated as follows:

$$\text{Yield}\,(\%) = \frac{W_2}{W_1} \times 100, \tag{1}$$

where W_1 is the initial weight of the precursor (g), and W_2 is the weight of the obtained biochar (g).

The biocarbons were characterized according to the method described in ASTM Standard D3172 (1997). Elemental analyzes of C, H and N were carried out by a Perkin Elmer model 2400 PECHN-SO analyzer using acetanilide as a reference. The oxygen content was obtained indirectly by difference. The thermal behavior was carried out with a Mettler-Toledo analyzer model TGA/SDTGA-851, under a nitrogen atmosphere, with a heat ramp of 10 ºC/min to 600 ºC. In addition, the biofuels were analyzed by Fourier transform infrared (FTIR) spectrophotometry on a Perkin Elmer Spectrum one spectrometer. Spectra were recorded in the region of 4000 to 370 cm^{-1}, resolution of 4 cm^{-1} and ten scans. The surface morphology of the precursors was observed by scanning electron microscopy (SEM) using a JEOL model JSM 6300 scanning electron microscope operated at 10 kV. For observation, the precursor particles were dispersed on carbon tape and plated with gold. By mercury porosimetry (Mp) in a Model AutoPore IV 9500 porosimeter with a detection range of 0.003 μm to 360 μm.

To determine the optimal contact time, samples of 0.2 g of each of the carbons obtained were added to 50 mL of a methylene blue (MB) solution with an initial concentration of 50 mg/L at pH = 8 and T = 22°C. The MB adsorption efficiency (% E) was calculated by Equation:

$$\%E = [(C_0 - C_t | C_0)] \times 100, \tag{2}$$

C_0 is the initial concentration of MB (mg/L), and C_t is the concentration of MB (mg/L) in the time t of contact (min). The amount of MB adsorbed or adsorption capacity (q_t, mg/L) at time t (min) for each experiment was calculated by Equation:

$$q_t = [(C_0 - C_t | W)] \times V. \tag{3}$$

Where q_t is the amount of MB adsorbed (mg/L) at time t (min), C_0 and C_t are the same as the previous ones, V is the experimental volume of the solution (L), and W is the weight of biochar used (g) (Ramírez *et al.*, 2016).

The Langmuir isotherm model establishes that adsorption occurs on a homogeneous surface by monolayer sorption without interaction between sorbed molecules (Hameed *et al.*, 2007; Bagheri & Abedi, 2009). In addition, the Langmuir model has certain assumptions such as: an adsorbent molecule occupies an adsorption site on a homogeneous surface; once all the adsorption sites are occupied the adsorbent is saturated since the adsorbate forms a single-molecule-thick surface (monolayer); there is no interaction between adjacent molecules of adsorbate (TAPPI, 1999). The linear form of the Langmuir isotherm equation is represented by Equation:

$$\frac{C_e}{q_e} = \frac{1}{Q_{\text{máx}} \times K_L} + \frac{C_e}{Q_{\text{máx}}}. \tag{4}$$

Where C_e (mg/L) is the concentration at equilibrium, q_e (mg/L) is the capacity of adsorption at equilibrium, $Q_{\text{máx}}$ is the maximum amount of adsorbate (mg/g) adsorbed at equilibrium when the adsorbent is saturated, and K_L is the Langmuir isotherm constant which is related to the affinity of the binding sites and the adsorption free energy (TAPPI, 1999; Weber *et al.*, 2010; Ramírez *et al.*, 2016).

3. RESULTS AND DISCUSSION

Results of physic-chemical characterization of the three residue materials are presented in Table 1. As shown, the moisture content of these residues was the same, around 7 %. Regarding this biomass constituent, Tripathi *et al.* (2016) mention that low moisture is advisable for the activated carbon production because it not only reduces the heat energy, but it also lowers the time required for the process. Specifically, lignocellulosic precursors with more than 30 % (Tripathi *et al.*, 2016); of moisture is not suitable for the pyrolysis since the greater amount of energy supplied to the biomass would be used in moisture removal present in it and rest would be used to increase its temperature. Added to this, large amount of moisture (more than 40 %) reduces the heating rate resulting in more time in achieving the process temperature (Tripathi *et al.*, 2016). In this sense, Demirbas (2004) and Xiong *et al.* (2013) observed that increase in moisture content in pyrolysis of wood and sewage sludge, respectively, decreases the yield of biochar. Thus, the moisture content of the three precursors of this study is suitable for the activated carbon production.

In contrast to the above mentioned, the literature indicates that the ash content is another important parameter in the activated carbon production since defines the quality of precursor in the combustion determining the content incombustible matter (Nieto-Delgado & Rangel-Méndez, 2013). Therefore, a low ash content is desired because it could negatively affect the yields to partially eliminate the formation of char (Pereira *et al.*, 2014; Tripathi *et al.*, 2016). In this research, the ash contents of precursors are less than 10 % and are acceptable for the activated carbons production which is in accordance with the result obtained by other studies as shown in Table 1.

Regarding the content of volatile matter, the literature mentions that this parameter is responsible for the pores in the structures of carbonaceous materials as precursors after being subjected to elevated temperatures

Table 1: Precursor chemical characterization [% w/w]

Precursor	Moisture	Ash	Fixed carbon	Volatile	Lignin	α-celullose
Barley husk	7.38 ± 0.05	7.91 ± 0.07	4.86	79.84 ± 0.10	26.46 ± 0.10	66.69 ± 0.04
Corn cob	6.91 ± 0.07	2.54 ± 0.02	6.09	84.46 ± 0.34	15.24 ± 0.03	52.60 ± 0.11
Agave leaves	6.50 ± 0.13	9.92 ± 0.05	10.65	79.30 ± 0.17	15.58 ± 0.15	79.45 ± 0.11
Precursor	**β- cellullose**	**γ-celulosa**	**Holocellulose**	**Sugars**	**Fat**	**Reference**
Barley husk	22.38 ± 0.02	10.92 ± 0.02	82.07 ± 4.81	27.44 ± 0.05	2.06 ± 0.03	This study
Corn cob	44.52 ± 0.13	2.89 ± 0.03	82.38 ± 3.27	19.34 ± 0.17	0.82 ± 0.01	This study
Agave leaves	13.18 ± 0.15	7.37 ± 0.03	83.05 ± 3.34	42.29 ± 0.16	1.68 ± 0.01	This study

the volatile material contained in it is released resulting in the formation of porous structures (Canales-Flores & Prieto-García, 2016). In this study, high volatile contents were found with values from 75 % to 80 %. These values are very suitable for the subsequent pyrolysis since the gradual and controlled release of volatile matter result in the enrichment of carbon in the precursor and furthermore are within the range reported for other similar precursors used in the preparation of activated carbons: 69-84 % (Canales-Flores & Prieto-García, 2016).

Therefore, the volatile matter content is another important parameter because it provides an indication of the reactivity and ease of ignition of an organic material. In the same way, fixed carbon, sugars and fat contents are similar to those reported in other studies.

Other criterion for the selection of the biomass, for the activated carbon production, is the lignin and cellulose content present in the raw material (Tripathi *et al.*, 2016).

Table 1 shows the contents of lignocellulosic compounds. α-cellulose contents from 52 % to 79 % were observed being agave leaves and barley husk which had the highest values. These results were superior to those reported in other studies as shown in Table 1. Such differences can be attributed to the extraction method used in this research, which is consistent with that reported by Espino *et al.* (2014) who conducted studies of chemical characterization of lignocellulosic materials as part of their investigation. On the other hand, β-cellulose contents of 44 % were obtained for corn cob while agave leaves and barley husk showed lower content, ranging 13-22 %. Meanwhile, γ-cellulose contents less than 11 % were determined. In contrast, high percentages of holocellulose of 82-83 % were found (the term holocellulose represents the total cellulose, which is composed of cellulose and hemicelluloses).

Another structural material is lignin whose content for barley husk was 26 % while agave leaves and corn cob had 15 %. The results obtained were consistent with those reported by (Ioannidou *et al.*, 2009; García & Rangel, 2009; Kaliyan & Morey, 2010; Kohli *et al.*, 2013; Espino *et al.*, 2014). From these results, it is shown that all of the biomass samples contain more cellulose than lignin. In this regard, Savova *et al.* (2001)

observed that the porosity of the produced biochar varies with the composition of cellulose and lignin and established that biomass with high lignin content produce biochar with macroporous structure while the plant biomass with high cellulose content produce biochar with microstructure. Therefore, knowledge of the values of lignocellulosic compounds is very important because the chemical composition of precursor has a direct influence on the properties of activated carbons, which is consistent with the findings of Pereira *et al.* (2014).

3.1. Elemental analyses

Biomass chemically is a complex composition of carbon, oxygen, hydrogen, nitrogen, sulfur, ash and small quantities of other elements such as alkali metals, alkali earth metals and heavy metals (Tripathi *et al.*, 2016). The chemical composition of biomass mainly depends on the type of biomass, growing condition and geographic location (Espino *et al.*, 2014; Tripathi *et al.*, 2016). Carbon, hydrogen, oxygen and nitrogen contents of precursors compared with other biomass are shown in Table 2. As shown, the content of carbon is the highest share in most of biomass which is followed by oxygen and then hydrogen. Regarding the carbon contents, barley husk, corn cob and agave leaves presented values close, ranging 42-45 %. The present finding also support Nieto-Delgado & Rangel-Méndez (2013) study which concluded that a good precursor of activated carbons should have a share of carbon in the range of 40-90 % (Nieto-Delgado & Rangel-Méndez, 2013).

The oxygen content of these biomass was the same, around 50 %. This share is followed by hydrogen content, around 6 %. In this sense, literature mentions that the proportion of carbon, oxygen and hydrogen is used to predict the heating value of the biomass and are the main contributors of the energy content in biomass (Tripathi *et al.*, 2016). Furthermore, it is seen from Table 2 that high carbon and oxygen contents is the characteristic of woody and agricultural residues. Thus, the presence of this elements in the lignocellulosic precursors leads to more char formation as well as to the high calorific value of the carbonaceous materials obtained (Tripathi *et al.*, 2016). In contrast nitrogen and sulfur are found in small found as shown in Table 2. Specifically, nitrogen was found in the precursors with values less than 1 % This result is favorable since high contents of nitrogen and sulfur in biomass result in the release of gas mixtures of SOx and NOx during pyrolysis of the biomass, which are toxic and are not environment friendly (Tripathi *et al.*, 2016). As shown, nitrogen content is very low in the precursors of this research, which provides evidence that pyrolysis of such precursor does not result in release of noxious gases. Thus, these findings also provide evidence that

Table 2: Carbon, oxygen, hydrogen, nitrogen and sulfur content [%] in biomass obtained from different sources

Biomass group	Biomass	Basis	C	O	H	N	S	Reference
	Barley husk	Dry and ash free	42.08	50.95	6.32	0.65	-	This study
	Corn cob	Dry and ash free	43.93	49.37	6.12	0.58	-	This study
	Agave leaves	Dry and ash free	44.63	49.52	5.83	0.02	-	This study

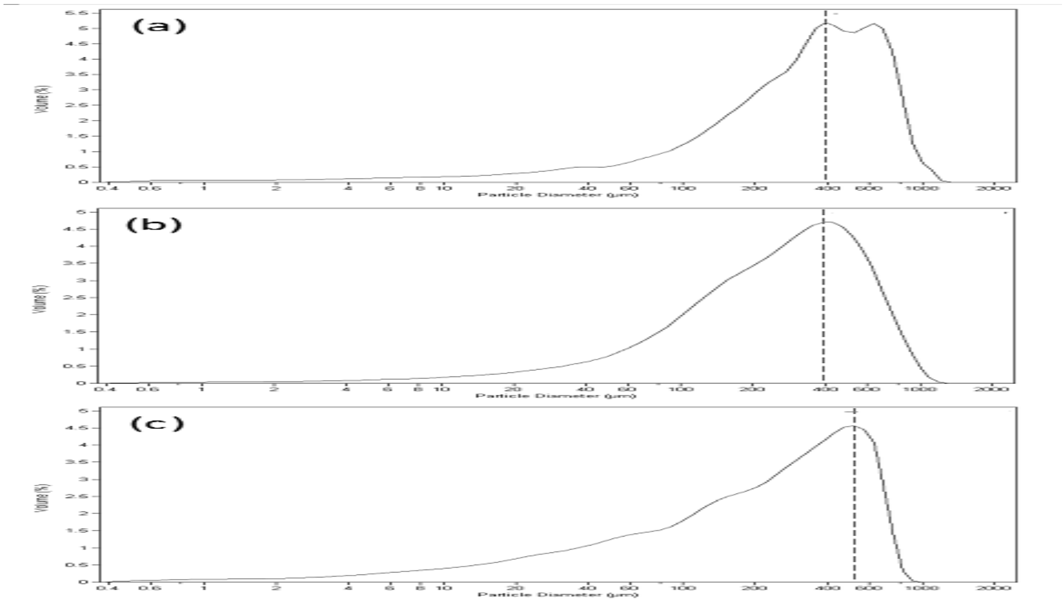

Figure 1: Particle size distribution of (a) barley husk, (b) corn cob and (c) agave leaves (Own elaboration)

raw materials examined in this study are good precursors for the production of activated carbons.

3.2. Particle size

Particles size is a factor which should be taken care in the activated carbon production as it can control the rate at which the heat is transferred to the input biomass (Tripathi *et al.*, 2016). Aislabi *et al.* (2013) indicates that particle size is a very important parameter in other processes of activated carbon preparation such as impregnation and activation. Figures 1a, 1b and 1c show of particle size distribution for barley husk, corn cob and agave leaves, respectively. Particle sizes in the range of 390.9-610.7 μm was observed in the precursor's materials. Specifically, corn cob had the smaller particle size to present a predominant mode of 390.9 μm. Particle sizes of 517.2 μm were observed in agave leaves. In contrast, the distribution curve of particle sizes for barley husk showed a bimodal behavior, observing values from 390.9 μm (most abundant) to 610.7 μm (less abundant). According to the literature, particle sizes of 0.250 to 2.000 mm are suitable to produce activated carbons (Canales-Flores & Prieto-García, 2016; Wu *et al.*, 2009; Aislabi *et al.*, 2013).
As shown, the particle size range of this study is within the range reported in the literature for other lignocellulosic precursors for activated carbon production.

Muller (2010) studied the effect of particle size on activated carbon adsorption. In this study, particle sizes in the ranges 63-100 μm, 100-250 μm, and 250-500 μm were examined. The results showed that the adsorption rate increased with decreasing particle size. Thus, the best adsorption results were obtained with particle sizes of 82 μm. Similar effects were observed by Sentorun-Shalaby *et al.* (2006) who examined the effect of

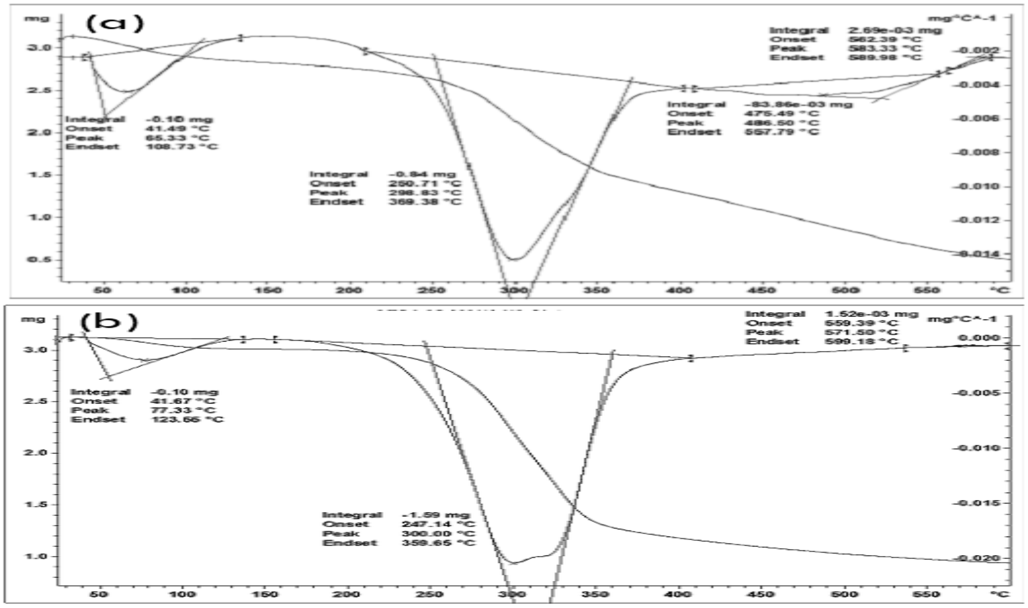

Figure 2: Termogravimetric analysis of (a) barley husk, (b) corn cob, (Own elaboration)

particle size on the properties of activated carbons. Three particle sizes were examined: 0.85 mm to 1.7 mm, 1.7 mm to 3.35 mm, and 3.35 mm to 4.00 mm. Their results revealed that the finer particles resulted in the development of larger surface areas and increased the percentage of micropores in the resulting activated carbons, which is a good agreement with the results of the present study. In contrast, Tripathi *et al.* (2016) added that although most of the reports show trend of high activated carbon yield on increasing particle size, few researchers have reported a reduction in the activated carbon yield on increasing the particle size of the lignocellulosic biomass. Therefore, the results of this study suggest that the particle sizes of precursors are suitable for the production of carbonaceous materials and are consistent with those shown in other research.

3.3. Thermogravimetry

As a representative result of the thermogravimetric analysis, Figures 2a, b y 3c show profiles of fraction of the mass decrease of combustibles for barley husk (Figure 2a), corb cob (Figure 2b) and agave leaves (Figure 3c). These profiles are compared with the profile of cellulose (Figure 3 d) since the biomass studied in this work mainly consist of this compound as show in Table 1. The vertical axis represents fraction of mass decrease of combustibles. From the figures, the thermal decomposition of lignocellulosic compounds starts at about 180 ºC for all the samples. According to the literature, the combustibles in the biomass react at the five stages during the thermal decomposition (Nieto-Delgado & Rangel-Méndez, 2013).

A first stage at temperature between 70°C and 150°C was observed which was attributed to moisture released and to the evaporation of some volatile compounds. The second stage (less pronounced than the previous one) was found from 180°C to about 230°C, and was attributed to the degradation of hemicellulose. This stage was only detectable by thermo-gravimetric analyzer in the agave leaves. At the third stage, the mass

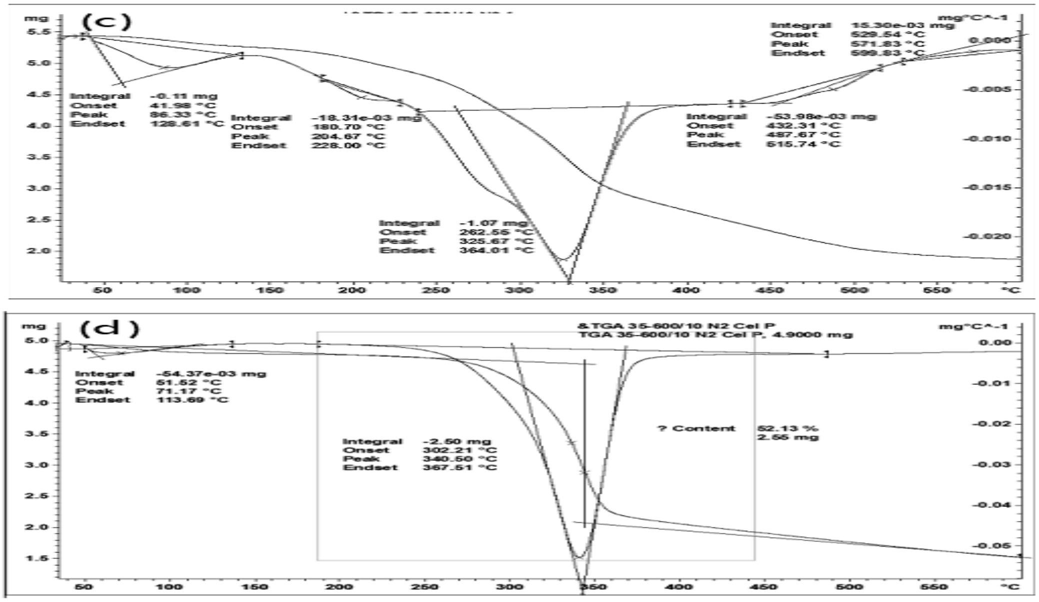

Figure 3: Termogravimetric analysis of (c) agave leaves, and (d) cellulose (Own elaboration)

rapidly decreases due to the cellulose volatilization. This main stage was observed in the temperature range of 250 ℃ to 350°C for all the samples, and was representative of the thermal decomposition of cellulose. Specifically, peaks at 299°C for barley husk, at 300°C for corn cob, and at 326°C for agave leaves were observed. Similar behaviors have been reported in other studies for the same precursors. For example, the profile DTGA of barley husk showed peaks for the thermal decomposition of cellulose at 245°C (Sentorun-Shalaby *et al.*, 2006) and 357°C (Li *et al.*, 2010), corn cob at 310°C (Bledzki *et al.*, 2010) and 340°C (Tsai *et al.*, 2001) and agave bagasse around 300°C (Nieto-Delgado & Rangel-Méndez, 2013) all obtained with heating rates of 10°C min^{-1} under nitrogen. After that, the slow mass decrease occurs at the fourth stage between 380 °C and 550°C due to lignin decomposition. Focusing on the pattern of the profile of mass decrease, trend of the mass decrease was similar at the third stage for all precursors. According to Gani & Naruse (2007), the cellulose decomposes at high decomposition rate within narrow temperature range, specifically 240-350°C (Nieto-Delgado & Rangel-Méndez, 2013).

In contrast, lignin is the biomass fraction with the higher decomposition temperature (280-500°C), is harder to decompose than the cellulose and the hemicellulose since part of lignin consists of benzene rings and is the fraction with higher carbon content (Nieto-Delgado & Rangel-Méndez, 2013; Gani & Naruse, 2007). Comparing these results for the biomass samples with those for the cellulose, the profiles for barley husk, corn cob and agave leaves approach to that for the cellulose (Figure 3 d). This is because the three precursors showed high cellulose content and low lignin content as shown in Table 1. Finally, the fifth stage was attributed to the ash derived from the degradation of complex polymers and inorganic salts present in the precursors, mainly in barley husk and agave leaves. These results are consistent with those reported by Gani

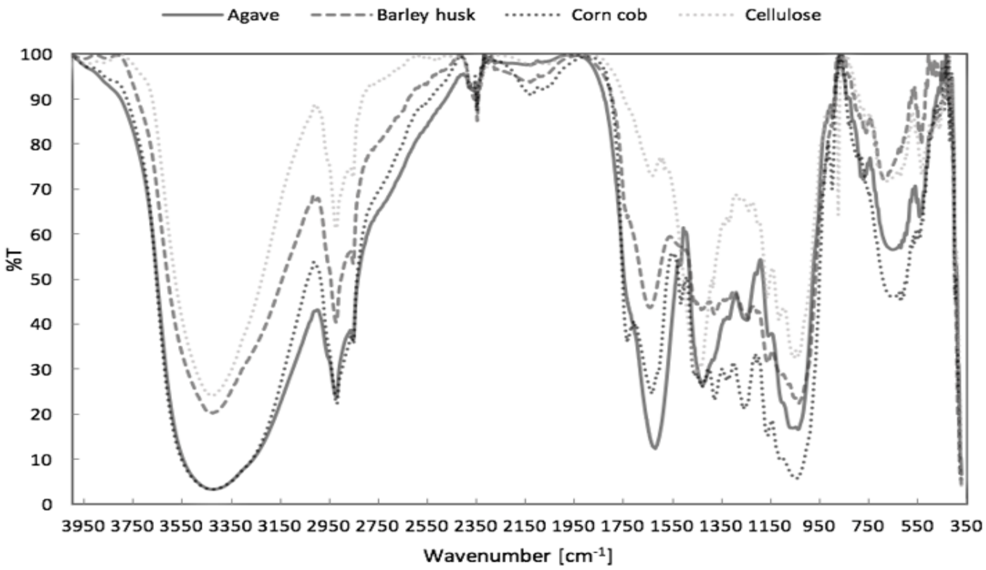

Figure 4: FTIR spectra of the residue materials (Own elaboration)

& Naruse (2007) who suggest that the thermal behavior of biomass depends on its own component such as the cellulose and lignin content. Additionally, these findings provide valuable information regarding the thermal decomposition (pyrolysis) of the precursors studied in this work.

3.4. Fourier-transform infrared spectroscopy (FTIR)

The FT-IR spectrum of the three precursors compared to cellulose is shown in Figure 4 and the assignment is given in Table 3. The peaks at 3425 cm^{-1} and 2919 cm^{-1} for barley husk, at 3425 cm^{-1} and 2918 cm^{-1} for corn cob, at 3424 cm^{-1} and 2919 cm^{-1} for agave leaves, and at 3435 cm^{-1} and 2923 cm^{-1} for cellulose were observed. The peak at about 3400 cm^{-1} is due to hydrogen bonded $O-H$ stretching. The hydrophilic tendency of the three precursors was reflected in the broad adsorption band, which is related to the $-OH$ groups present in aliphatic or aromatic alcohol and present in their main components. The peak at around 2900 cm^{-1} is due to the $C-H$ asymmetric and symmetric stretching from aliphatic saturated compounds. These two stretching peaks are corresponding to the aliphatic moieties in cellulose and hemicellulose (Skoulou & Zabaniotou, 2007).

The peak at 2346 cm^{-1} was observed for the three precursors and at 2353cm^{-1} for cellulose. On the other hand, the peaks at 2106 cm^{-1} for barley husk, at 2108 cm^{-1} for corn cob, at 2102 cm^{-1} for agave leaves, and at 2111 cm^{-1} for cellulose were observed. The sharp peaks at around 2340cm^{-1} are attributed to the $P-H$ stretching and $P-O-H$. The band at about 2112 cm^{-1} is attributed to the $Si-H$ stretching. According to Bledzki *et al.* (2010), the bands of this region are representative of inorganic hydride or oxide. In the double

Table 3: Attribution of the bands presented in the FTIR spectra

		Biomass		Peak location	Attribution
Barley husk	Corn cob	Agave leaves	Cellulose	range (cm^{-1})	
3425	3425	3424	3435	3460-3400	$O-H$ stretching
2919	2918	2919	2923	3000-2850	$C-H$ asymmetric and symmetric stretching in methyl and methylene group
2346	2346	2346	2353	2400-2300	$P-H$ stretching and $P-O-H$ stretching
2106	2108	2102	2111	2200-2100	$Si-H$ stretching
1733	1737	1731	1722	1738-1700	$C=O$ stretching in acetyl and uronic ester groups or in carboxylic group of ferulic and cumaric acids
1656	1643	1635	1635	1650-1580	$N-H$ bending in primary amine
1386	1383	1396	1344	1375-1350	$C-H$ rocking in alkanes or $C-H$ stretching in methyl and phenolic alcohol
1251	1266	1265	1241	1250-1200	$Si-CH_2$ stretching alkane or $C-C$ plus $C-O$ plus $C=O$ stretching
1053	1063	1062	1055	1086-1030	$C-H$ in plan deformation plus $C-O$ deformation in primary alcohol

bond region, a shoulder peak at 1733 cm^{-1} for barley husk, at 1737 cm^{-1} for corn cob, at 1731 cm^{-1} for agave leaves and a peak at 1722 cm^{-1} for cellulose were assigned to the $C=O$ stretching of the acetyl and uronic ester groups of hemicellulose or to the ester linkage of carboxylic group of the p-cumaric acid of lignin. The sharp peaks at 1656 cm^{-1} for barley husk, at 1643 cm^{-1} for corn cob, and at 1635 cm^{-1} for agave and cellulose, are corresponding to amide I. The bands in the range 1375-1350 cm^{-1} were assigned from the $C-H$ symmetric and asymmetric deformations in methyl and phenolic alcohol. In the band region of 1250-1200 cm^{-1} represents $Si-CH_2$ stretching in alkane or $C-C$ plus $C-O$ plus $C=O$ stretching and deformation bands in cellulose and lignin (Li *et al.*, 2010). Barley husk, corn cob, agave leaves and cellulose showed an absorption peak at 1053 cm^{-1} , 1063 cm^{-1} , 1062 cm^{-1} , and 1055 cm^{-1} , respectively. The peak in the range 1086-1030 cm^{-1} was assigned to $C-O$ deformation in secondary alcohol and aliphatic ether. A sharp peak at around 900 cm^{-1} is representative of of the $C-1$ group frequency or ring frequency and is characteristic of β-glycosidic linkages between the sugar units (Sentorun-Shalaby *et al.*, 2006). In this sense, peaks at 908 cm^{-1} for barley husk, at 899 cm^{-1} for corn cob, at 917 cm^{-1} for agave leaves, and at 873 cm^{-1} for cellulose were observed.

As can be seen, the content of chemical components was similar but with different peak areas. In addition, FTIR spectrum were diffuse with a strong overlap of the peaks. The spectral differences were not well defined, which can be attributed to the high complexity of the various types of intermolecular and intramolecular interactions present in the lignocellulosic residues.

3.5. Scanning electron microscopy (SEM)

Figures 5 a-c show the surface morphology of the raw material of barley husk, corn cob and agave leaves, respectively. It can be observed that three lignocellulosic residues have fibrous and porous structure, which are suitable characteristics to obtain carbonaceous materials such as activated carbons (Canales-Flores &

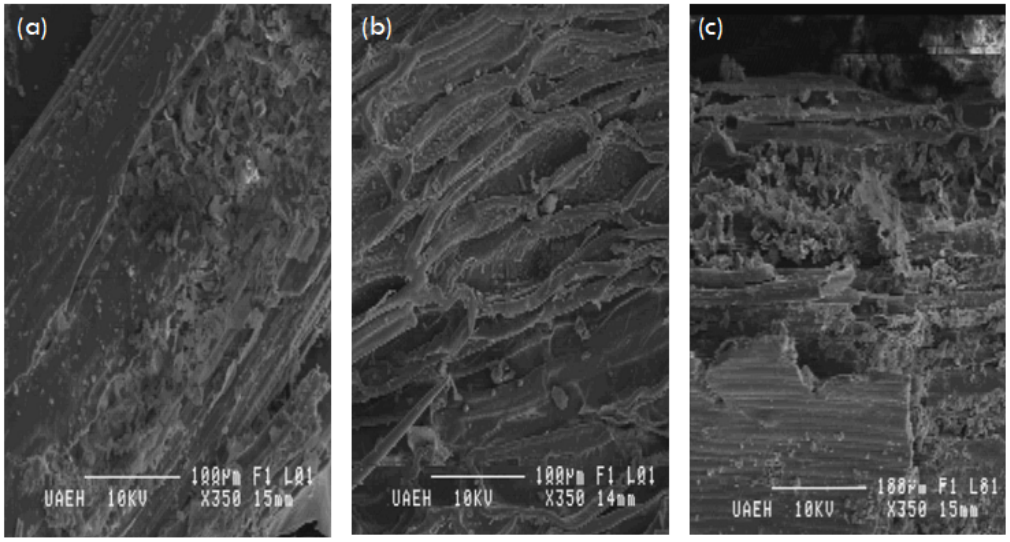

Figure 5: Morphology of (a) barley husk, (b) corn cob, and (c) agave leaves (Own elaboration)

Prieto-García, 2016), since biomass can easily decompose and burn. According to the literature, a good precursor of activated carbon must have a porous and fibrous structure, since under this condition, the oxygen can easily diffuse inside the particle during combustion, and volatile material can be gradually released. In addition, the combustion reactivity of lignocellulosic residues deeply relates to the activated carbon morphology formed (Gani & Naruse, 2007). From this observation results, the three residues materials can be potential precursors of activated carbons.

3.6. Mercury porosimeter (Mp)

Figure 6 presents the pore size distribution obtained by Mp of the surfaces of the three samples. Three main regions can be seen: one between 0.01 and 1 μm; another between 2 and 10 μm; and a third between 50 and 300 μm. These regions are attributed to the interconnections between the pores and to the small pores formed by aeration. Factors that can influence an underestimation of pore size, and its distribution, may be due to the allocation of the diameter of the observed surface in comparison with the micrographs (SEM), or to a misinterpretation of the interconnections as diameters of spherical pores. All these considerations can lead to a pore size measurement and analysis smaller than actual size, leading to a non-sample pore size distribution curve. The high volatile contents (75-80 %, in Table 1) are very suitable values for gradual and controlled release by pyrolysis. Therefore, it provides an indication of the reactivity and ease of ignition of an organic material and formation of pores. The development of porosity is explained from a double phenomenon; first, narrow micropores are created, then these narrow micropores grow to produce larger pores broad becoming meso and macropores.

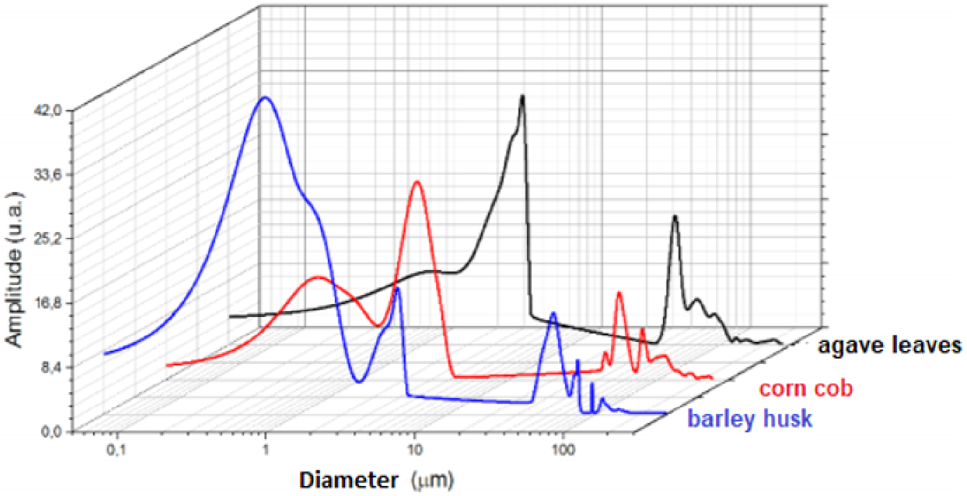

Figure 6: Analytical curves obtained by adding the deconvolutions ($R^2 > 0.99$) of the pore size distribution characterized by Mp: (blue) barley husk, (red) corn cob, and (black) agave leaves (Own elaboration)

3.7. Obtaining biocarbons

Yields between 16 and 34 % were obtained for BHB, between 3 and 18 % for CCB and between 15 and 39 % for ALB. The literature also mentions that the effect of carbonization time is directly related to other process parameters, such as carbonization temperature and heating rate. The carbonization temperature increases the yield of biochar to 400 ºC. This carbonization temperature was the best to obtain the highest carbon yields, since the high temperatures promote the thermal cracking of the heavy carbohydrates present in the precursor, increasing the liquid and gaseous products, and the decrease in the biochar yield (Tripathi *et al.*, 2016); Rangabhashiyam & Balasubramanian (2019) also reported the decrease of the biochar yield with increasing pyrolysis temperature. It was indicated that the three precursors had high α-cellulose contents and low lignin contents. The literature indicates that, during pyrolysis processes, low temperatures are suitable for cellulose because at high temperatures (> 800°C) cellulose leads to the formation of volatile products while at low temperatures (450-600°C), leads to the formation of biochar, since cellulose degrades to anhydrocellulose resulting in a high production of biochar. Therefore, the carbonization temperature of 400 ºC was adequate to obtain higher biochar yields.

3.8. Characterization of the biochars obtained

A comparison of the results of the proximal analysis of biofuels in comparison with the precursors is seen in Figure 7. The moisture content of the precursors was the same, around 7 %, and for biofuels less than 4 %. Tripathi *et al.* (2016) mention that low humidity is advisable to produce activated carbon because it not only reduces thermal energy but also reduces the time required for the process. Specifically, lignocellulosic

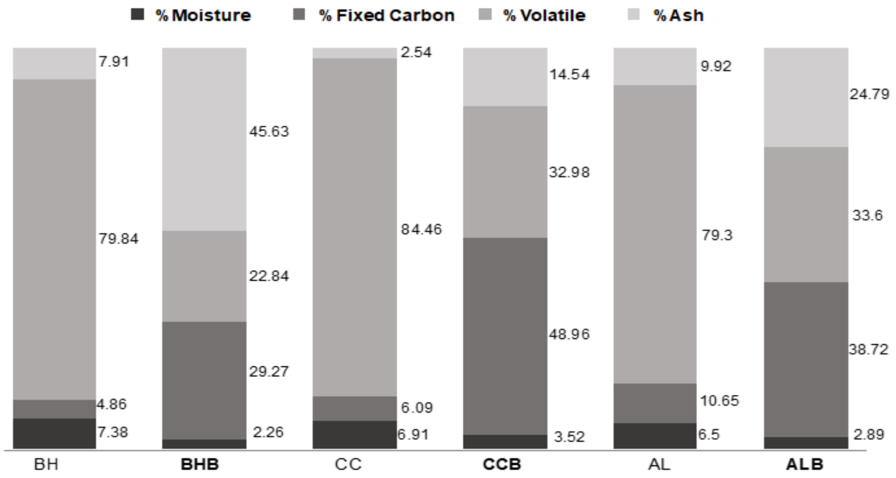

Figure 7: Proximal analysis of biochars obtained and precursors. (Own elaboration)

precursors with more than 30 % humidity are not suitable for pyrolysis since the greater amount of energy contributed to the biomass would be used to eliminate the humidity present in it and the rest would be used to increase its temperature.

Ash content is another important parameter in the activated carbon production since it defines the quality of precursor in the combustion determining the content of incombustible matter and it is related to the dissolution of salts generating problems of pollution in aqueous media when the activated carbon is used (Nieto-Delgado & Rangel-Méndez, 2013); Thus, a low ash content is desired because it could negatively affect the yields to partially eliminate the formation of char (Pereira *et al.*, 2014); FTIR spectra of the BH compared with BHB, CC compared with CCB, and AL compared with ALB are shown in Figure 8A-C. The intense and is appearing at 3400 cm^{-1} in all samples, was attributed to stretching vibrations, characteristic of the hydroxyl functional group $(O-H)$ belonging to the cellulose structure, which is the major component of the precursors. The band characteristic of the methyl group resultant of $(C-H)$ asymmetric and symmetric stretching was assigned to olefinic compounds, which suggests an aliphaticity in the structure of the precursors. It was observed that the three precursors present diverse functional groups such as esters, ethers, alcohols, aldehydes, ketones, phenols, and carboxylic acids. Thus, in the double bond region, a shoulder peak at 1733 cm^{-1} for BH, at 1737 cm^{-1} for CC, and at 1731 cm^{-1} for AL, were assigned to the C=O stretching of the acetyl and uronic ester groups of hemicellulose, and to the ester linkage of carboxylic group of the p-coumaric acid of lignin. These bands disappeared in the spectra of the three biochars (Figure 8A-C). On the contrary, it can be observed that there are few differences on the peak assigned to primary amines both in precursors and in biofuels. This explains a peak at 1626 cm^{-1}

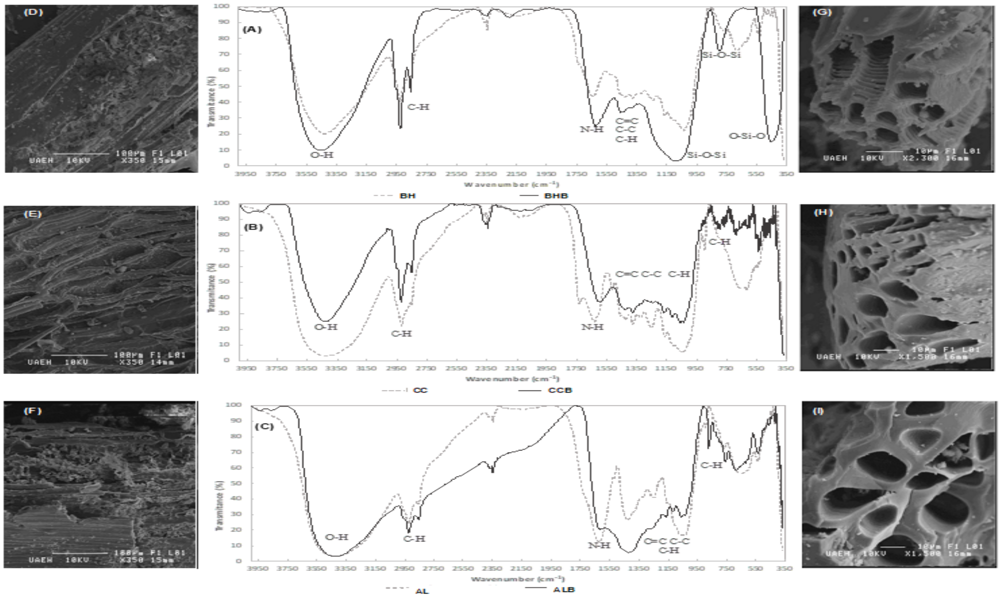

Figure 8: FTIR spectrum of biochars compared with the precursors (A, B, and C). SEM micrographs of precursors (D, E, and F) and biochars (G, H, and I). (Own elaboration)

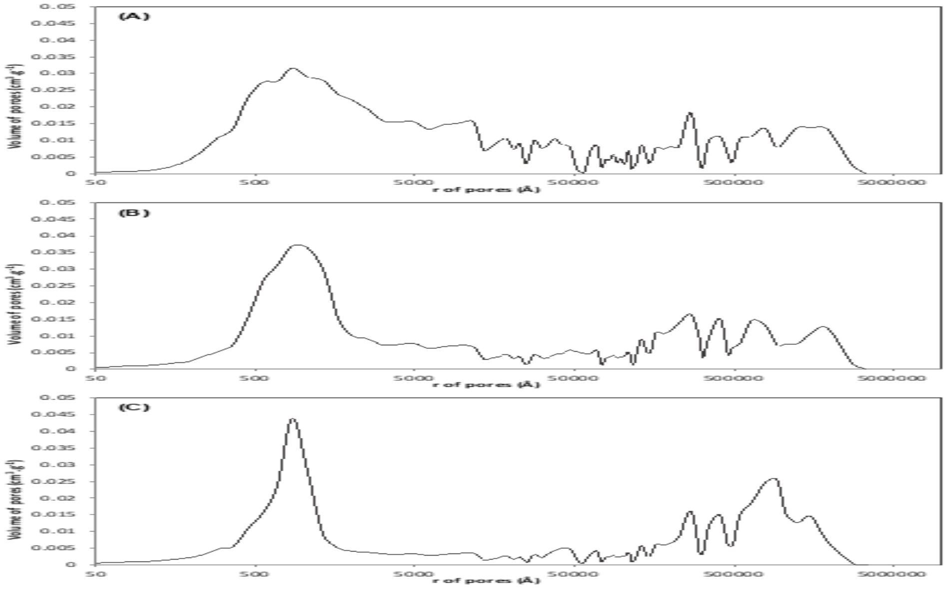

Figure 9: Pore size distribution curve for (A) BHB, (B) CCB, and (C) ALB. (Own elaboration)

(more intense) for BHB (Figure 8A), at 1595 cm^{-1} (low intensity) for CCB (Figure 8B) and at 1612 cm^{-1} (shoulder) for ALB (Figure 8C) were observed. SEM is also compared.

Figure 9 shows the pore size distribution curves for BHB, CCB and ALB. The pore sizes were classified

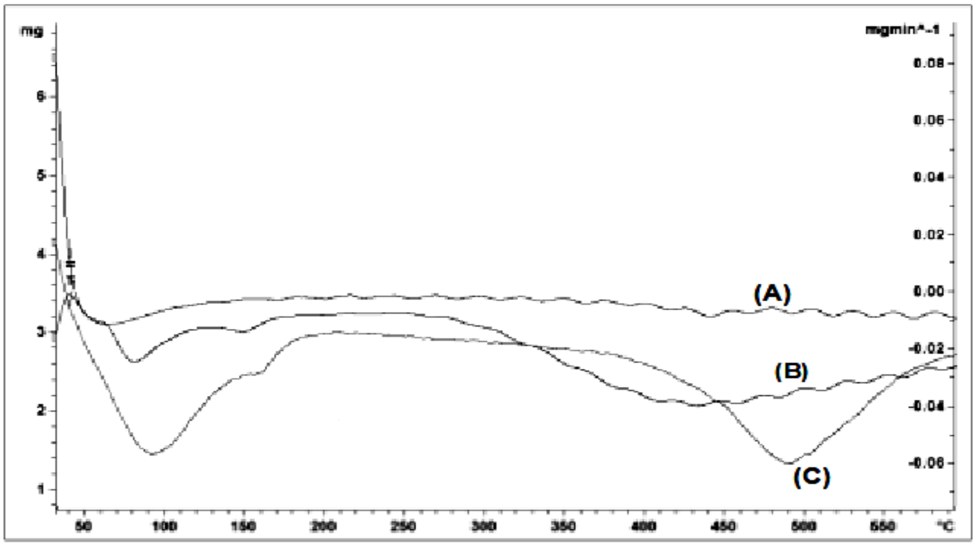

Figure 10: Thermogravimetric analysis of (A) BHB, (B) CCB, and (C) ALB. (Own elaboration)

according to the pore radius (micropores 1-20 Å, mesopores 20-500 Å, macropores 500-50000 Å). When we compared the pore size distribution curves for the three biofuels, we observed the predominance of macroporous structures in the three materials. ALB presented the highest macropore volume with 0.045 cm3/g, followed by CCB with 0.037 cm^3/g and BHB with 0.031 cm^3/g. Therefore, biocarbons with macroporous structures were obtained under pyrolysis conditions.

Figure 10 shows profiles of the mass decrease fraction for biofuels. In the thermal decomposition profile of the biocars, a very discrete endothermic peak was observed at temperatures below 100°C, attributed to the desorption of the physiosorbed water. For the biochars sample, the peak corresponding to the degradation of cellulose and hemicellulose was not observed. It is a difference with respect to the thermal decomposition profile of lignocellulosic residues. Finally, fluctuations that occur between 450 and 550°C were found in the thermal decomposition profile of the biochars that can be attributed to the prolonged degradation of lignin since this compound has a high thermal stability. This peak was more intense in ALB since its precursor has the highest lignin content.

Figures 11 a-b show graphs of experimental adsorption capacity [qe (mg/g)] and removal efficiency (% E) of MB, respectively. The kinetic results show that equilibrium was reached at 180 min in all cases. Thus, Figure 10-a shows that the material that obtained the highest adsorption capacity was ALB with 103.02 mg/g, followed by BHB with 98.18 mg/g and CCB with 89.26 mg/g. Figure 11-b show that ALB is the material with the highest removal efficiency of MB with 80.41%, followed by BHB with 74.66%, and CCB with 71.41%. After the activation process, the capacity and the adsorption efficiency increased considerably for

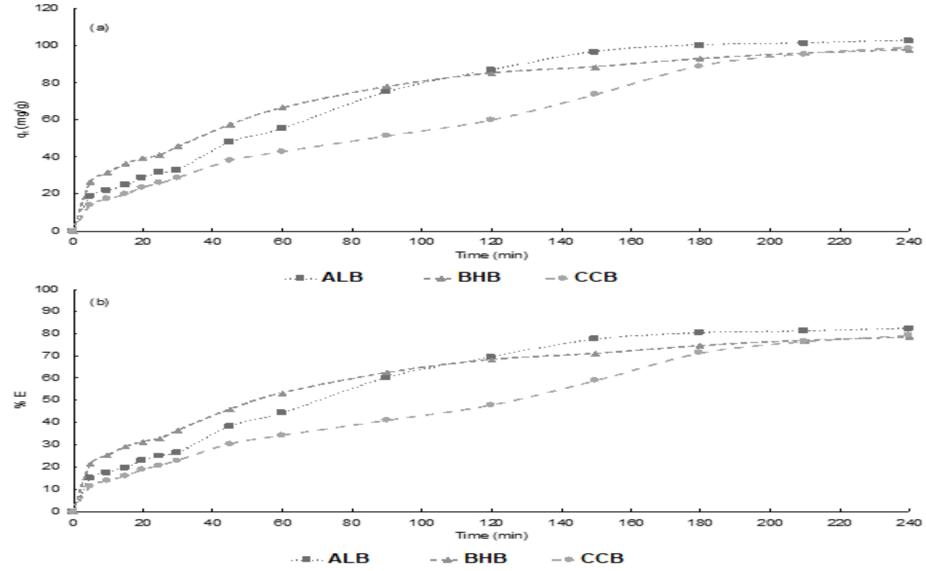

Figure 11: Kinetics of MB obtained with 0.2 g of adsorbent, initial concentration of 50 mg/L, a particle diameter of 1.5-0.25 mm, pH=8, and T=22°C. (Own elaboration)

the three adsorbents since they require less time to reach equilibrium. It can be observed that after the chemical activation process assisted by microwaves, the capacity and the efficiency of adsorption were increased considerably for ALB and CCB; however, these parameters decreased for ALB. This behavior is because the microwave assisted activation method has the effect of increasing the C/O ratio by eliminating functional groups that contain acid oxygen. The agave biochar is the one with the highest content of these functional groups. Therefore, under the experimental conditions, microwaves modify the oxygenated functionalities mainly in the ALB. For this reason, the active sites of this material decrease considerably (oxygenated groups mainly), which results in the reduction of the adsorption capacity and removal efficiency of MB.

In relation to ALB, there is a significant increase in its adsorption capacity. This finding is attributed to possible interactions of inorganic elements in the amorphous silicon oxides and other metal oxides present in ALB, which can cause an effect catalytic. This condition favors the formation of polycyclic aromatic systems (increases the C/O ratio) and consolidation of well-developed porous structures with many oxygenated active sites as observed in the IR spectrum of ALB.

4. CONCLUSION

The analysis of lignocellulosic compounds shown that holocellulose and cellulose were the main fractions, obtaining the trend agave leaves > barley husk > corn cob. In contrast, lignin content was low, for barley husk agave leaves and corn cob. Elemental analysis showed that agave was the precursor to the higher carbon content, followed by corn cob and barley husk, which is within the range reported in the literature for optimal precursors of activated carbons. This ratio was followed by the oxygen content and the hydrogen content; the ash content was low ($< 10\,\%$) and the volatile content was high ($75\,\%$ to $80\,\%$). These values are very suitable for the subsequent pyrolysis since the gradual and controlled release of volatile matter result in the enrichment of carbon in the precursor. The analysis of the particle size distribution curves showed values that are within the range reported in the literature for other lignocellulosic precursors to produce activated carbon. Thermogravimetric analysis showed similar thermal decomposition profiles of lignocellulosic compounds, with cellulose being the main stage for all samples, with peaks around 300°C. The findings from this study make several contributions to the literature. First, the properties of the biomass such as moisture, cellulose, lignin and particle size, are the main parameters to be considered for choosing a good precursor of activated carbon. The second major finding was that precursors of this study showed high levels cellulosic fractions in the profiles of thermal decomposition. Therefore, it provides that temperatures in the range of decomposition of cellulose are most suitable to promote the formation of char, to obtain high yields of product, and get important properties of porosity and surface after the subsequent activation processes. From these findings, it is established that barley husk, corn cob and agave leaves can be considered as potential precursors of activated carbons. Finally, this research will serve as a base for future studies of thermal decomposition of this precursor. It should be noted that these findings should be complemented with the study of other parameters related to the production of activated carbons. Additionally, it is recommended that further research be undertaken in the pyrolysis and activation areas of this lignocellulosic residues.

References

Aislabi, T. M., Abustan, I., Ahmad, M. A. & Foul, A. A. (2013). A review: production of activated carbon from agricultural byproducts via conventional and microwave heating. *J Chem Technol Biotechnol*, 88, 1183-1190. doi: 10.1002/jctb.4028

ASTM Standard D3172 (1997). Standard practice for proximate analysis of coal and coke. ASTM International, West Conshohocken, PA.

ASTM Standard D3173 (1996). Standard test method for moisture in the analysis sample of coal and coke. ASTM International, West Conshohocken, PA.

ASTM Standard D3174 (2000). Standard test method for ash in the analysis sample of coal and coke from coal. ASTM International, West Conshohocken, PA.

ASTM Standard D3175 (1997). Standard test method for volatile matter in the analysis sample of coal and coke. ASTM International, West Conshohocken, PA.

Azevedo-Carvalho, A. F., de Oliva-Neto, P., Fernandes-da Silva, D. & Maria-Pastore, G. (2013). Xylo-oligosaccharides from lignocellulosic materials: Chemical structure, health benefits and production by chemical and enzymatic hydrolysis. *Food Res Int* 51, 75–85. doi: 10.1016/j.foodres.2012.11.021

Bagheri, N. & Abedi, J. (2009). Preparation of high surface area activated carbon from corn by chemical activation using potassium hydroxide. *Chem Eng Res Des*, 87, 1059-1064. doi: 10.1016/j.cherd.2009.02.001

Bledzki, A. K., Mamum, A. A. & Volk, J. (2010). Barley husk and coconut shell reinforced polypropylene composites: The effect of fibre physical, chemical and surface properties. *Compos Sci Technol*, 70, 840. doi: 10.1016/j.compscitech.2010.01.022

Cagnon, B. P. X., Guillot, A., Stoeckli, F. & Chambat, G. (2009). Contributions of hemicellulose, cellulose and lignin to the mass and the porous properties of chars and steam activated carbons from various lignocellulosic precursors. *Bioresource Technol*, 100, 292-298. doi: 10.1016/j.biortech.2008.06.009

Canales-Flores, R. A. & Prieto-García, F. (2016). Activation Methods of Carbonaceous Materials Obtained from Agricultural Waste. *Chem Biodiversity*, 13, 261-268. doi: 10.1002/cbdv.201500039

Demirbas, A. (2004). Effect of initial moisture content on the yields of oily products from pyrolysis of biomass. *J Anal Appl Pyrol*, 71, 803-815. doi: 10.1016/j.jaap.2003.10.008

Espino, E., Cakir, M., Domenek, S., Román-Gutiérrez, A. D., Belgacem. N. & Bras, J. (2014) Isolation and characterization of cellulose nanocrystals from industrial by-products of Agave tequilana and barley. *Ind Crop Prod*, 62, 552-559. doi: 10.1016/j.indcrop.2014.09.017

Gani, A. & Naruse, I. (2007). Effect of cellulose and lignin content on pyrolysis and combustion characteristics for several types of biomass. *Renew Energ*, 32, 649-661. doi: 10.1016/j.renene.2006.02.017.

García-Reyes, R. B. & Rangel-Mendez, J. R. (2009). Contribution of agro-waste material main components (hemicelluloses, cellulose, and lignin) to the removal of chromium (III) from aqueous solution. *J Chem Technol Biotechnol*, 84, 1533-1538. doi: 10.1002/jctb.2215

Hameed, B. H., Ahmad, A. L.& Latiff, K. N. A. (2007). Adsorption of basic dye (methylene blue) onto activated carbon prepared from rattan sawdust. *Dyes and Pigments*, 75, 143-149.

Ioannidou, O., Zabaniotou, A., Antonakou, E. V., Papazisi, K. M., Lappas, A. A. & Athanassiou, C. (2009). Investigating the potential for energy, fuel, materials and chemicals production from corn residues (cobs and stalks) by non-catalytic and catalytic pyrolysis in two reactor configurations. *Renew Sust Ener Rev*, 13, 750-762. doi: 10.1016/j.rser.2008.01.004

Kaliyan, N. & Morey, R. (2010). Densification characteristics of corn cobs.*Fuel Process Technol*, 91, 559-565. doi: 10.1016/j.fuproc.2010.01.001

Khezami, L., Chetouani, A., Taouk, B. & Capart, R. (2005). Production and characterisation of activated carbon from wood components in powder: Cellulose, lignin, xylan. *Powder Technol*, 157, 48-56. doi: 10.1016/j.powtec.2005.05.009

Kohli, D., Garg, S. & Jana, A. K. (2013). Thermal and morphological properties of chemically treated barley husk fiber. *Int J Res Mech Eng Technol*, 3, 153-156.

Li, H., Foston, M. B., Kumar, R., Samuel, R., Gao, X., Hu, F., Ragauskas, A. J. & Wyman, C. E. (2010). Chemical composition and characterization of cellulose for Agave as a fast-growing, drought-tolerant biofuels feedstock. *RSC Adv*, 2, 4951-4958. doi: 10.1039/C2RA20557B

Muller, B. R. (2010). Effect of particle size and surface area on the adsorption of albumin-bonded bilirubin on activated carbon. *Carbon*, 48, 3607-3615. doi: 10.1016/j.carbon.2010.06.011

Nieto-Delgado, C. & Rangel-Méndez, J. R. (2013). Preparation of Carbon Materials from Lignocellulosic Biomass. In: Rufford TE (ed) Green Carbon Materials. Advanced and Aplications, Taylor & Francis Group, US, pp 51.

Pereira, R. G., Martins, C., Mendes, N., Farias, L., Ferreira, R. C., Oliveira, A., Oliveira, M. & da Costa, R. (2014). Preparation of activated carbons from cocoa shells and siriguela seeds using H_3PO_4 and $ZnCl_2$ as activating agents for BSA and α-lactalbumin adsorption. *Fuel Process Technol*, 126, 476-486. doi: 10.1016/j.fuproc.2014.06.001

Ramírez, A. P., Giraldo, S., Flórez, E. & Acelas, N. (2016). Preparation of activated carbon from palm oil wastes and their application for methylene blue removal. *Revista Colombiana de Química*, 46 (**1**), 33-41.

Rangabhashiyam, S. & Balasubramanian, P. (2019). The potential of lignocellulosic biomass precursors for biochar production: Performance, mechanism and wastewater application –A review. *Industrial Crops and Products*, 128, 405-423. https://doi.org/10.1016/j.indcrop.2018.11.041

Savova, D., Apak, E., Ekinci, E., Yardim, F., Petrov, N., Budinova, T., Razvigorova, M. & Minkova, V. (2001). Biomass conversion to carbon adsorbents and gas. *Biomass Bioenerg*, 21, 133-142. doi: 10.1016/S0961-9534(01)00027-7

Sentorun-Shalaby, C., Artok, L. & Sarici, C. (2006). Preparation and characterization of activated carbons by one-step steam pyrolysis/activation from apricot stones. *Micropor Mesopor Mat*, 88, 126-134. doi: 10.1016/j.micromeso.2005.09.003

Skoulou, V. & Zabaniotou, A. (2007). Investigation of agricultural and animal wastes in Greece and their allocation to potential application for energy production. *Renew Sustain Energ Rev*, 11, 1698-1719. doi: 10.1016/j.rser.2005.12.011

Stefanidis, S. D., Kalogiannis, K. G., Iliopoulou, E. F., Michailof, C. M., Pilavachi, P. A. & Lappas, A.A. (2014). A study of lignocellulosic biomass pyrolysis via the pyrolysis of cellulose, hemicellulose and lignin. *J Anal Appl Pyrol*, 105, 143-150. doi: 10.1016/j.jaap.2013.10.013

TAPPI T203 (1999). Alpha-, beta- and gamma-cellulose in pulp. TAPPI Press, Norcross, Georgia.

TAPPI T204 (1997). Solvent extractives of wood and pulp. TAPPI Press, Norcross, Georgia.

TAPPI T222 (1998). Acid-insoluble lignin in wood and pulp. TAPPI Press, Norcross, Georgia.

Tripathi, M., Shahu, J. N. & Ganesan, P. (2016). Effect of process parameters on production of biochar from biomass waste through pyrolysis: A review. *Renew Sust Ener Rev*, 55, 467-481. doi: 10.1016/j.rser.2015.10.122

Tsai, W. T., Chang, C. Y., Wang, S. Y., Chang, C. F., Chein, S. F. & Sun, H. F. (2001) Cleaner production of carbon adsorbents by utilizing agricultural waste corn cob. *Resour Conserv Recy*, 32, 43-53. doi:10.1016/S0921-3449(00)00093-8

Weber, E., Fernandez, M. & Wapner, P. (2010). Comparison of X-ray micro-tomography measurements of densities and porosity principally to values measured by mercury porosimetry for carbon–carbon composites. *Carbon*, 48(**8**), 2151–2158. https://doi.org/10.1016/j.carbon.2009.11.047

Wise, L.E., Marphy, M. & d 'Adieco, A. (1946). A chlorite holocellulose, its fractionation and bearing on summative wood analysis and studies on the hemicelluloses. *Pap Trade J*, 122, 35-43.

Wu, Y., Wu, S., Li, Y. & Gao, J. (2009). Physico-chemical characteristics and mineral transformation behavior of ashes from crop straw. *Energ Fuels*, 23, 5144-5150. doi: 10.1021/ef900496b

Xiao, H., Peng, H., Deng, S., Yang, X., Zhang, Y. & Li, Y. (2012). Preparation of activated carbon from edible fungi residue by microwave assisted K_2CO_3 activation–Application in reactive black 5 adsorption from aqueous solution. *Bioresource Technol*, 111, 127-133. doi: 10.1016/j.biortech.2012.02.054

Xiong, S., Zhuo, J., Zhang, B. & Yao, Q. (2013). Effect of moisture content on the characterization of products from the pyrolysis of sewage sludge. *J Anal Appl Pyrol*, 104, 632-639. doi: 10.1016/j.jaap.2013.05.003